PHYSICAL REVIEW C, VOLUME 65, 061301(R)

Effective interaction for pf-shell nuclei

M. Honma
Center for Mathematical Sciences, University of Aizu, Tsuruga, Ikki-machi, Aizu-Wakamatsu, Fukushima 965-8580, Japan

T. Otsuka
Department of Physics, University of Tokyo, Hongo, Tokyo 113-0033, Japan
and RIKEN, Hirosawa, Wako-shi, Saitama 351-0198, Japan

B. A. Brown
National Superconducting Cyclotron Laboratory and Department of Physics and Astronomy, Michigan State University, East Lansing, Michigan 48824-1321

T. Mizusaki
Institute of Natural Sciences, Senshu University, Higashimita, Tama, Kawasaki, Kanagawa 214-8580, Japan
(Received 17 October 2001; revised manuscript received 19 April 2002; published 31 May 2002)

An effective interaction is derived for use in the full pf basis. Starting from a realistic G-matrix interaction, 195 two-body matrix elements and four single-particle energies are determined by fitting to 699 energy data in the mass range 47–66. The derived interaction successfully describes various structures of pf-shell nuclei. As examples, systematics of the energies of the first 2^+ states in the Ca, Ti, Cr, Fe, and Ni isotope chains and energy levels of ^{56,57,58}Ni are presented. The appearance of a new magic number 34 is seen.

DOI: 10.1103/PhysRevC.65.061301 PACS number(s): 21.60.Cs, 21.30.Fe, 27.40.+z, 27.50.+e

The nuclear shell model has been very successful in our understanding of nuclear structure: once a suitable effective interaction is found, the shell model can reproduce/predict various observables accurately and systematically. For light nuclei, there are several ''standard'' effective interactions such as the Cohen-Kurath [1] and the USD [2] interactions for the p and sd shells, respectively. On the other hand, in the next major shell, i.e., in the pf shell, a unified effective interaction for all nuclei in this region has not been available. The pf shell is quite important for a variety of problems in nuclear structure, such as the stability/softness of the magic number 28, and nuclear astrophysics, such as electron capture in supernovae explosions. Thus, a sound, systematic, and precise description of the pf-shell nuclei is urgent and important. In this paper, we present a unified effective interaction which one can apply to the shell-model description of the entire pf shell.

The spin-orbit splitting gives rise to a sizable energy gap in the pf shell between the $f_{7/2}$ orbit and the other orbits ($p_{3/2}$, $p_{1/2}$, $f_{5/2}$), producing the N or $Z=28$ magic number. However, the excitations across the gap are important for ground- and excited-state properties of many pf-shell nuclei. It is intriguing to understand how this magic number persists or fades away in various situations. We shall discuss this point in this paper, and the word ''cross-shell'' refers to the N or $Z=28$ shell gap hereafter. Because of such cross-shell mixing, shell-model calculations including all pf-shell configurations are necessary, and the predictive power obtained with a unified effective interaction in the full pf-shell space is very important. The full pf-shell calculation, however, leads to the diagonalization of huge Hamiltonian matrices with dimensions of up to two billion. The extreme difficulty of dealing with such large matrices is the major reason why a unified effective interaction has been missing for the pf shell. The Monte Carlo shell model (MCSM) introduced recently [3,4] has changed the situation by making such calculations feasible over the entire region of the pf shell. Also conventional shell-model calculations have advanced.

The effective interaction can in principle be derived from the free nucleon-nucleon interaction. In fact such microscopic interactions have been proposed for the pf shell [5,6] with certain success particularly in the beginning of the shell. These interactions, however, fail in cases of many valence nucleons, e.g., ^{48}Ca [6] and ^{56}Ni.

These microscopic interactions can be modified empirically so as to better reproduce experimental data. The monopole-modified interaction, KB3 [7], and also the shell-gap readjusted version, KB3G [8], appear to be quite successful in the lower pf shell ($A \leqslant 52$). But these modifications turn out to be insufficient for a consistent description of the cross-shell properties: e.g., the 2_1^+ level of ^{56}Ni with KB3G is predicted about 2 MeV higher than the observed value.

The FPD6 interaction [9] is of another type: an analytic two-body potential was assumed with parameters determined by a fit to the experimental data of $A=41\sim49$ nuclei. It successfully describes heavier pf-shell nuclei, such as ^{56}Ni and ^{64}Ge [3,4]. There are, however, some defects, for instance, in the single-particle aspects of ^{57}Ni.

We now turn to our new interaction. An effective interaction for the pf shell can be specified uniquely in terms of interaction parameters consisting of four single-particle energies ϵ_a and 195 two-body matrix elements $V_{JT}(ab;cd)$, where $a,b,\ldots$ denote single-particle orbits, and JT stand for the spin-isospin quantum numbers. Although ϵ_a's include kinetic energies as well, they are treated as a part of the effective interaction as usual. We adjust the values of the interaction parameters so as to fit experimental binding en-

ergies and energy levels. We outline the fitting procedure here, while details can be found in Ref. [10]. For a set of N experimental energy data $E^k_{\rm exp}$ $(k=1,\ldots,N)$, we calculate corresponding shell-model eigenvalues λ_k's. We minimize the quantity $\chi^2=\Sigma^N_{k=1}(E^k_{\rm exp}-\lambda_k)^2$ by varying the values of the interaction parameters. Since this minimization is a nonlinear process with respect to the interaction parameters, we solve it in an iterative way with successive variations of those parameters followed by diagonalizations of the Hamiltonian until convergence.

Experimental energies used for the fit are limited to those of ground and low-lying states. Therefore, certain linear combinations (LC's) of interaction parameters are sensitive to those data and can be well determined, whereas the rest of the LC's are not. We then adopt the so-called LC method [11], where the well-determined LC's are separated from the rest: starting from an initial interaction, well-determined LC's are varied by the fit, while the other LC's are kept unchanged (fixed to the values given by the initial interaction).

In order to obtain shell-model energies, both the conventional and MCSM calculations are used. Since we are dealing with global features of the low-lying spectra for essentially all pf-shell nuclei, we use a simplified version of MCSM: we search a few (typically three) most important basis states (deformed Slater determinants) for each spin parity, and diagonalize the Hamiltonian matrix in the few-dimensional basis approximation (FDA). The energy eigenvalues are improved by an empirical correction formula with parameters fixed by cases where more accurate results are available. This is called hereafter few-dimensional approximation with empirical corrections (FDA*), which actually yields a reasonable estimate of the energy eigenvalues with much shorter computer time.

In the selection of experimental data, in order to eliminate intruder states from outside the present model space, we consider nuclei of $A\geqslant 47$ and $Z\leqslant 32$. As a result 699 data of binding and excitation energies (490 yrast, 198 yrare and 11 higher states) were taken from 87 nuclei: $^{47-51}$Ca, $^{47-52}$Sc, $^{47-52}$Ti, $^{47-53,55}$V, $^{48-56}$Cr, $^{50-58}$Mn, $^{52-60}$Fe, $^{54-61}$Co, $^{56-66}$Ni, $^{58-63}$Cu, $^{60-64}$Zn, ^{62,64,65}Ga, and ^{64,65}Ge. We assume an empirical mass dependence $A^{-0.3}$ of the two-body matrix elements similarly to the USD interaction [2]. We start from the realistic G-matrix interaction with core-polarization corrections based on the Bonn-C potential [6], which is simply denoted G hereafter. 70 well-determined LC's are varied in the fitting procedure, and a new interaction GXPF1 was obtained with a rms error 168 keV within FDA*.

The first 2^+ energy level of even-even nuclei is a good systematic measure of the structure. The left panel of Fig. 1 shows them for the Ca, Ti, Cr, Fe, and Ni isotopes. The lightest nucleus in each isotope chain corresponds to $N=Z$ because of the mirror symmetry. The energies are computed by FDA* and by exact or nearly exact conventional shell-model calculations by the code MSHELL [12]. The former gives a reasonable approximation to the latter, while the differences are up to 0.2 MeV. The overall description of the 2^+ levels is quite successful throughout these isotope chains. In all cases, the energy jump corresponding to $N=28$ shell closure is nicely reproduced.

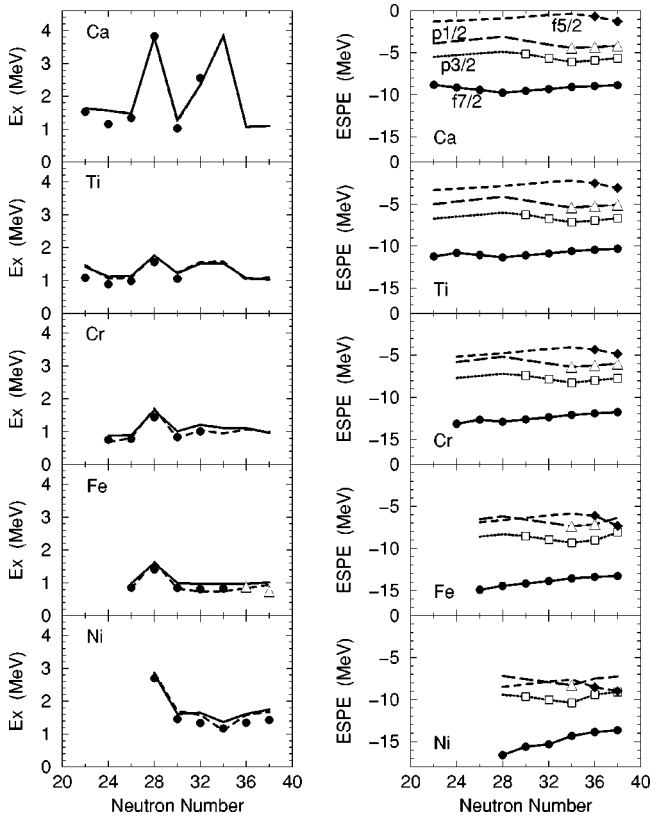

FIG. 1. (Left) First 2^+ levels as a function of the neutron number N. Experimental data are shown by filled circles [13] and open triangles [14]. Solid lines show results of conventional calculations: the maximum number of nucleons excited from $f_{7/2}$ to $p_{3/2}$, $p_{1/2}$ or $f_{5/2}$ is five for ^{56}Fe and ^{58,60,62}Ni, six for ^{52,54}Fe and ^{56}Ni, and seven for ^{58,60}Fe, whereas the others are exact. Dashed lines imply FDA* results. (Right) Effective single-particle energies for neutron orbits. Symbols indicate that the corresponding orbit is occupied by at least one nucleon in the lowest filling configuration.

A basic aspect of the effective interaction is provided by the effective single-particle energy (ESPE) [7,15]. The ESPE depends on the monopole part of the Hamiltonian, and reflects angular-momentum-averaged effects of the two-body interaction for a given many-body system. In the right panel of Fig. 1, ESPE's of the neutron orbits are shown. A new $N=34$ magic structure has been predicted in Ref. [16]. In fact a large energy gap ($\sim$4.1 MeV) between $p_{1/2}$ and $f_{5/2}$ can be seen in the ESPE for Ca and Ti isotopes.

As predicted also in Ref. [16], due to the large attractive proton-neutron matrix elements, the ESPE of the $\nu f_{5/2}$ orbit comes down as $\pi f_{7/2}$ orbit is occupied, reducing this subshell gap. One can indeed see this change in Fig. 1: the $N=34$ subshell becomes weaker in Cr, and disappears in Fe and Ni. This means that the $N=34$ magic number arises only in neutron-rich Ca and Ti isotopes, and is gone in stable nuclei. On the other hand, the ESPE's of Ni isotopes in Fig. 1 indicate that the $f_{5/2}$, $p_{3/2,1/2}$ orbits are degenerate to a good extent, forming a subshell that resembles a degenerate pseudo-sd shell. This fact may be relevant in constructing

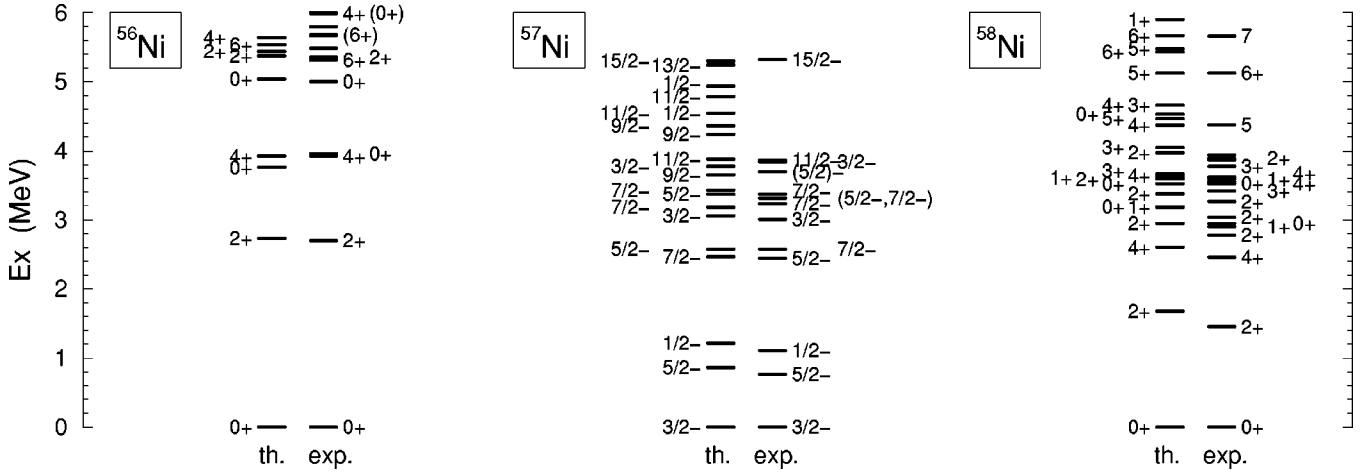

FIG. 2. Energy levels of ^{56,57,58}Ni. Experimental data are taken from Ref. [13]. Above 4 MeV, experimental levels are shown only for yrast states for ^{57,58}Ni.

some algebraic models, for instance, a pseudo-SU(4) of IBM-4 [17].

In the Ca isotopes, a prominent peak in the calculated 2^+ excitation energy can be seen at $N=34$, which is as high as that of the doubly magic nucleus ^{48}Ca. This is exactly due to the $N=34$ subshell closure discussed above. Note that this calculation is a result of the diagonalization of the Hamiltonian, whereas the ESPE reflects only its monopole part. The subshell gap at $N=32$ is much smaller ($\sim$1.6 MeV) between $p_{3/2}$ and $p_{1/2}$, and shows less pronounced effect in a consistent manner with experiment. The gap at $N=34$ is not large with the FPD6 interaction as can be inferred from the 2^+ state systematics shown in Fig. 4 of Ref. [18]. Thus the experimental energy of the 2^+ state in ^{54}Ca will be an important test of the pf-shell Hamiltonians.

In the Ni isotopes, both experimental and theoretical 2^+ excitation energies drop at $N=34$, where ESPE of $\nu p_{1/2}$ and $\nu f_{5/2}$ are almost degenerate and therefore the collectivity is enhanced. It is remarkable that the drastic change of the structure among those nuclei can be described by a single effective interaction. Toward the end of the pf shell ($N=40$), effects of $g_{9/2}$ seem to appear.

The nucleus ^{56}Ni is a challenge for a unified description of nuclei in the cross-shell region of the pf shell. The stability of the $(f_{7/2})^{16}$ core plays important roles, while most of existing effective interactions fail in reproducing certain properties related to the core softness. In Fig. 2 energy levels of ^{56,57,58}Ni are shown. Theoretical levels are obtained by MCSM calculations, where typically 13 J-compressed basis states [4] are taken for each state. These MCSM calculations are more accurate than the FDA*. The agreement between the theory and the experiment is satisfactory.

In the calculated spectrum of ^{56}Ni, the deformed band discussed in Refs. [19,20] appears as 0_3^+, 2_2^+, 4_4^+, 6_3^+, ... In the yrast band, we obtain $B(E2;0_1^+\rightarrow 2_1^+)=5.5\times 10^2\ e^2\mathrm{fm}^4$, while in the deformed band, $B(E2;0_3^+\rightarrow 2_2^+)=1.8\times 10^3\ e^2\mathrm{fm}^4$. Here, effective charges, $e_p=1.23$, $e_n=0.54$, are taken [4]. The former $B(E2)$ value is in agreement with experiment [21]. The probability of the $(f_{7/2})^{16}$ configuration in the ground state is 69%. This value is larger than that obtained by FPD6 (49%) [4], while is smaller than the corresponding quantity for ^{48}Ca (94% for GXPF1).

In order to study the core softness, we made a rather ''soft'' interaction (GXPF2). For 20 matrix elements of the type $V_{JT}(aa;bc)$ where $a=f_{7/2}$ and $b,c\neq a$, we keep their G interaction values. We then carried out a fit for 60 best determined LC's, and came up with a rms error of 188 keV for 623 data within FDA*. This means that the fit is only slightly worse (by $\sim$20 keV) than GXPF1. The probability of $(f_{7/2})^{16}$ configuration in the ground state of ^{56}Ni is 49% suggesting its softness. Thus the energy data included in the fit can be reproduced about equally well within certain allowance of the softness. The core property, however, is important for certain observables. For example, the total Gamow-Teller strength from the ground state is calculated as $B(GT_+)=11.3$ (9.5) for GXPF1 (GXPF2). Since this is 13.7 for the closed shell, one sees the degree of the quenching which can be crucial in the electron capture in the supernovae explosion. From the KB3, one obtains 10.1 [22].

In the lowest three states $3/2^-$, $5/2^-$, and $1/2^-$ of ^{57}Ni, the $(f_{7/2})^{16}$ core is broken similarly to ^{56}Ni ground state, and these are ''single-particle'' states built on top of the correlated ^{56}Ni ground state. Their relative positions are determined mainly by the ESPE's. In pf-shell nuclei, in general, the cross-shell excitations occur rather commonly in low-lying states [23]. In ^{57}Ni, states above the three ''single-particle'' states contain further cross-shell excitations, which provide a good testing ground for cross-shell two-body matrix elements. A similar situation has been seen in ^{56}Ni particularly for its $4p$-$4h$ deformed band, while such effects are less evident in ^{58}Ni, with an exception of the 0_3^+ state which contains a sizable amount of proton $2p$-$2h$ excitations [24]. In these examples np-nh refers to the particle-hole excitations across the gap on top of the correlated ground state [23]. A comprehensive picture for such a wide variety of states requires the full-space calculations with an appropriate effective interaction.

The description of odd-A nuclei is also an important test of the interaction. We again consider Ni isotopes as examples, for which energy levels of yrast $1/2^-$, $3/2^-$, and

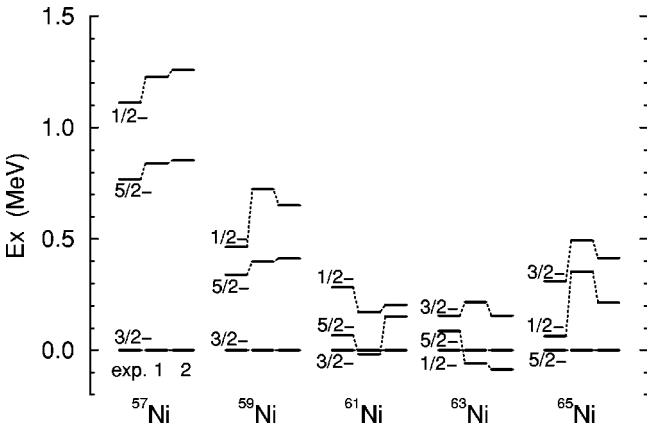

FIG. 3. Energy levels of odd-A Ni isotopes. Experimental data are taken from Ref. [13]. Theoretical results are calculated by using GXPF1/2 interactions, which are indicated as 1 and 2, respectively. Shell model calculations were carried out by the code MSHELL [12]. The results for $^{57-63}$Ni are obtained with truncating the number of nucleons excited from $f_{7/2}$ orbit up to six, whereas the result for ^{65}Ni is exact.

$5/2^-$ states are shown in Fig. 3. Experimentally, as the number of neutrons increases, both $1/2^-$ and $5/2^-$ states come down relative to $3/2^-$ level, forming nearly degenerate states around ^{63}Ni. This characteristic feature is nicely reproduced by both GXPF1/2 interactions. The downward slope of $5/2^-$ level, however, seems to be somewhat too steep, especially in GXPF1, which leads to some deviations within about 0.2 MeV, while the basic degeneracy around ^{63}Ni is clearly maintained. Since the results of the FDA* used in the fit are much closer to experimental spectra, a part of this deviation is due to the uncertainty in the FDA*.

These yrast levels contain similar amount of cross-shell excitations within each isotope. In fact, the occupation number of $f_{7/2}$ orbit varies from 15.0 (14.6) for ^{57}Ni to 15.6 (15.5) for ^{65}Ni by GXPF1 (GXPF2), while the difference among the lowest three states within each isotope is less than 0.3. Therefore the core excitation appears to play a minor role for describing relative energies of these lowest three levels. However, it should be emphasized that the GXPF1/2 interactions can describe these lowest levels as well as non-yrast levels for which the cross-shell excitation is essential.

In usual shell-model interactions, we often take the single-particle energies ϵ_a from experimental energy spectra of the one-particle/hole system on top of the assumed inert core. In the case of pf shell, many existing effective interactions such as KB3 borrow them from ^{41}Ca. However, our main purpose is not to describe light pf-shell nuclei from the beginning of the shell, but to treat cross-shell excitations over N or $Z=28$ shell gap. Therefore, in the present approach, we have assumed single-particle energies as parameters and determined them by the fit.

In Table I the single-particle energies relative to $p_{3/2}$ orbit are shown for various interactions. It is remarkable that the single-particle energy spacing between $f_{7/2}$ and $p_{3/2}$ orbits in GXPF1/2 interactions is enhanced by about 0.9 MeV in comparison to the energy spectrum of ^{41}Ca (or KB3). This difference in single-particle energies results from the exclusion

TABLE I. Single-particle energies relative to $p_{3/2}$ of various interactions.

Orbit	KB3	FPD6	GXPF1	GXPF2
$f_{7/2}$	−2	−1.8924	−2.9447	−2.8504
$p_{1/2}$	2	2.0169	1.5423	1.6054
$f_{5/2}$	4.5	4.5986	4.2964	4.2584

of energy data of $A<47$ nuclei from the fit. The wave functions of nuclei near ^{40}Ca contain relatively large amounts of intruder state admixtures, and the sd shell should be included in their description. A fit in which the single-particle energies are fixed to their values in ^{41}Ca is possible, but the total rms error in the energies becomes larger. The ESPE of GXPF1 interaction for Ca isotopes becomes very close to that of KB3, which is known to be quite successful for light pf-shell nuclei, already around $A\sim45$ (where the difference is less than 0.2 MeV). Thus the description of $A<47$ nuclei by GXPF1/2 interactions is still reasonable and similar to that of KB3, except for the those nuclei at the very beginning of the shell.

In Fig. 4(a), a comparison between GXPF1 and G is shown for the 195 two-body matrix elements. One finds a strong correlation. On average, the $T=0$ ($T=1$) matrix elements are modified to be more attractive (repulsive). The majority of most attractive matrix elements are $T=0$ ones, and, in particular, the two most attractive ones belong to $T=0$ $f7f5$ in both GXPF1 and G, where the notation $f7f5$ refers to the set of matrix elements $V_{J,T}(ab;ab)$ with $a=f_{7/2}$, $b=f_{5/2}$.

In Fig. 4(b) the difference between GXPF1 and G is shown for several $T=0$ diagonal matrix elements. The fit makes them more attractive. Although the $f7f7$ matrix elements are dominated by the monopole shift, i.e., a J-independent correction, the corrections to cross-shell matrix elements $f7p3$ and $f7f5$, become larger for higher J's. Such J dependences beyond the monopole shifts are of interest. The same feature is also found in GXPF2. Apart from these corrections, notable differences between G and GXPF1

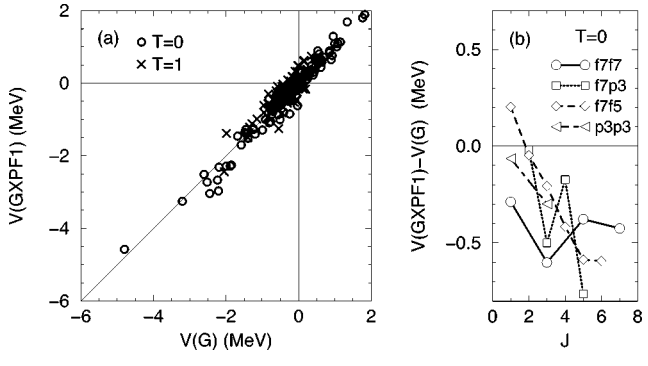

FIG. 4. (a) Correlation of $V_{JT}(ab;cd)$ between G and GXPF1. $T=0$ and $T=1$ matrix elements are shown by open circles and crosses, respectively. (b) Difference of diagonal $T=0$ matrix elements between G and GXPF1 as a function of the angular momentum J coupled by two nucleons.

are found in the $T=1$ monopole-pairing cross-shell matrix elements.

In summary, a new unified pf-shell effective interaction, GXPF1, has been obtained. The GXPF1 interaction has monopole properties enforced by the energy data, and it properly handles cross-shell excitations, leading to a successful description of structure of Ni isotopes. Corrections beyond the monopole shifts are important. The systematic behavior of the energies for the lowest 2^+ levels of even-even nuclei are in good agreement with experiment, suggesting that collective properties are well described. We investigated the possible range of the softness of $N=Z=28$ core, coming up with another interaction, GXPF2. The applications to unexplored regimes of large neutron numbers or high excitation energy is of great interest. For example, the GXPF1 interaction demonstrates the appearance of a new magic number $N=34$ [16] in neutron-rich nuclei. Future experiments will test the predictions and provide guidance for further improvements in the Hamiltonian.

The authors thank M. Hjorth-Jensen for providing us the interaction matrix elements. A part of the numerical calculations were carried out by a parallel computer, Alphleet at RIKEN. This work was supported in part by a Grant-in-Aid for Scientific Research [Grant No. (A)(2)(10304019)], and by a Grant-in-Aid for Specially Promoted Research (Grant No. 13002001), and by the U.S. National Science Foundation Grant No. PHY-0070911.

[1] S. Cohen and D. Kurath, Nucl. Phys. **73**, 1 (1965).
[2] B. A. Brown and B. H. Wildenthal, Ann. Rev. Nucl. Part. Sci. **38**, 29 (1988).
[3] M. Honma, T. Mizusaki, and T. Otsuka, Phys. Rev. Lett. **75**, 1284 (1995); **77**, 3315 (1996).
[4] T. Otsuka, M. Honma, and T. Mizusaki, Phys. Rev. Lett. **81**, 1588 (1998).
[5] T.T.S. Kuo and G.E. Brown, Nucl. Phys. **A114**, 241 (1968).
[6] M. Hjorth-Jensen, T.T.S. Kuo, and E. Osnes, Phys. Rep. **261**, 125 (1995).
[7] A. Poves and A.P. Zuker, Phys. Rep. **70**, 235 (1981).
[8] A. Poves, J. Sánchez-Solano, E. Caurier, and F. Nowacki, Nucl. Phys. **A694**, 157 (2001).
[9] W.A. Richter, M.G. van der Merwe, R.E. Julies, and B.A. Brown, Nucl. Phys. **A523**, 325 (1991).
[10] M. Honma, B. A. Brown, T. Mizusaki, and T. Otsuka, Nucl. Phys. **A704**, 134 (2002).
[11] W. Chung, Ph.D. thesis, Michigan State University, 1976.
[12] T. Mizusaki, RIKEN Accel. Prog. Rep. **33**, 14 (2000).
[13] *Table of Isotopes*, edited by R. B. Firestone *et al.* (Wiley, New York, 1996).
[14] M. Hannawald *et al.*, Phys. Rev. Lett. **82**, 1391 (1999).
[15] Y. Utsuno, T. Otsuka, T. Mizusaki, and M. Honma, Phys. Rev. C **60**, 054315 (1999).
[16] T. Otsuka *et al.*, Phys. Rev. Lett. **87**, 082502 (2001).
[17] O. Juillet, P. Van Isacker, and D.D. Warner, Phys. Rev. C **63**, 054312 (2001).
[18] J.I. Prisciandaro *et al.*, Phys. Lett. B **510**, 17 (2001).
[19] T. Mizusaki, T. Otsuka, Y. Utsuno, M. Honma, and T. Sebe, Phys. Rev. C **59**, R1846 (1999).
[20] D. Rudolph *et al.*, Phys. Rev. Lett. **82**, 3763 (1999).
[21] G. Kraus *et al.*, Phys. Rev. Lett. **73**, 1773 (1994).
[22] K. Langanke and G. Martinez-Pinedo, Phys. Lett. B **436**, 19 (1998).
[23] T. Mizusaki, T. Otsuka, M. Honma, and B.A. Brown, Phys. Rev. C **63**, 044306 (2001).
[24] H. Nakada, T. Sebe, and T. Otsuka, Nucl. Phys. **A571**, 467 (1994).